Supporting Information for "Weddell Sea control of ocean temperature variability on the western Antarctic Peninsula"

Adele K. Morrison[1], Matthew H. England[2], Andrew McC. Hogg[3], Andrew E. Kiss[3]

[1]Research School of Earth Sciences and Australian Centre for Excellence in Antarctic Science, Australian National University, Canberra, 2601, Australia.

[2]Climate Change Research Centre and Australian Centre for Excellence in Antarctic Science, University of New South Wales, Sydney, 2052, Australia.

[3]Research School of Earth Sciences and ARC Centre of Excellence for Climate Extremes, Australian National University, Canberra, 2601, Australia.

Contents of this file

Introduction The supporting information provides additional information about the ACCESS-OM2-01 model configuration (Text S1), the observational analysis shown in Fig-

---

Corresponding author: A. K. Morrison, Research School of Earth Sciences, Australian National University, Canberra, 2601, Australia. (adele.morrison@anu.edu.au)

ure 1 (Text S2), the calculation of Dense Shelf Water formation (Text S3) and statistical analysis (Text S4).

Text S1: Model Configuration

The ocean component of ACCESS-OM2-01 is MOM5.1 (Griffies, 2012) and the sea ice component is CICE5.1.2 (Hunke et al., 2012). The model does not include tides or ice shelf cavities.

The historical simulation used is the third repeated 61 year cycle forced by JRA55-do (version 1.4) from 1958-2018, which is described and evaluated extensively in Solodoch et al. (2022). The first cycle is initialised from World Ocean Atlas 2013 v2. At the end of the first and second cycles, the forcing snaps back to the year 1958, following the Ocean Model Intercomparison Project phase 2 (OMIP-2) protocol (Tsujino et al., 2020). We exclude the years 1958-1962 of the third cycle from the analysis to limit the impact of rebound from the looping of the atmospheric forcing from the previous cycle.

For the repeat year forced control simulation, a single year of JRA55-do (version 1.3) is used to force the model and is repeated over and over. The 12 month period from May 1990 to April 1991 is used due to the neutral state of several climate indices (e.g. ENSO, SAM) (Stewart et al., 2020). The repeat year control simulation provides a very stable baseline configuration with no interannual variability from which perturbation experiments may be branched off. The control simulation was spun up for 250 years prior to the 12 year analysis period used in this study.

The passive tracer used to quantify connectivity is linearly restored to a value of 1 in the surface grid cell in the hatched region in Figure 2a, with a time scale of 1000 s. The passive tracer in the control run is initialised to zero in the interior after the 250 year spinup. The passive tracer is then forced at the surface and evolves passively in the ocean interior via advection and diffusion for 12 years. The passive tracer release region was chosen to incorporate all of the Dense Shelf Water formation in the Weddell Sea, based on the spatial distribution of the surface watermass transformation diagnostic. The passive tracer used in the historical run, which is only used in Figure S5, is also restored back to 0 at the surface outside the release region, in order to focus on Dense Shelf Water pathways originating only in the south-west Weddell Sea. The passive tracer in the repeat year forced control and perturbation simulations does not have any restoring outside the tracer release region.

Text S2: Observational Comparison

Hydrographic data from instrumented seals are used to evaluate the model's representation of the temperature distribution over the western Antarctic Peninsula continental shelf (Figure 1a). This analysis is performed on a depth slice at 206 m, because this is the model depth where we see the maximum temperature anomaly due to the Weddell Sea connectivity mechanism (see Figure 3d). Data is sourced from the Marine Mammals Exploring the Oceans Pole to Pole (MEOP-CTD) database (Treasure et al., 2018). We use the adjusted data, which has corrections applied based on comparisons with historical CTD and Argo data (Roquet et al., 2011). The estimated uncertainty on the calibrated data is ± 0.02°C for temperature. A profile is included in the analysis if a) the location is polewards of the 1000 m isobath (based on the model's bathymetry), b) salinity, pressure and temperature data are all available, and c) the maximum depth in the profile is at least 206 m. This results in 42213 profiles spanning the period 2005 - 2015. Observed in situ temperature is converted to conservative temperature and interpolated to the same depth as the model temperature data (206 m) for comparison. Interpolated profiles are binned onto a 0.4° longitude by 0.15° latitude grid.

Model profiles are selected from monthly averaged output of the historical simulation in the same month and at the nearest model grid point to the observed profiles. Extracted model profiles are then spatially binned using the same method applied to the observed profiles.

Text S3: Dense Shelf Water Formation Analysis

The Dense Shelf Water formation rate shown in Figure 1c (orange line) is calculated using the surface water mass transformation metric, following the method of Newsom, Bitz, Bryan, Abernathey, and Gent (2016). Dense Shelf Water formation is defined as the surface transformation that occurs poleward of the 1000 m isobath in the orange region shown in Figure 1d, across a density of $\sigma_0 = 1027.83\,\mathrm{kg\,m^{-3}}$ (i.e. surface waters lighter than $1027.83\,\mathrm{kg\,m^{-3}}$ transforming into waters denser than $1027.83\,\mathrm{kg\,m^{-3}}$ due to the action of surface heat and freshwater fluxes). Frazil heat fluxes are included in the surface heat flux for the calculation, even though they can occur beneath the surface layer. The surface water mass transformation metric is computed using monthly averaged model output.

The density threshold ($\sigma_0 = 1027.83\,\mathrm{kg\,m^{-3}}$) for the Dense Shelf Water formation calculation is chosen to be slightly denser than the density of the peak time-averaged surface water mass transformation (see Figure S5a). The chosen density threshold correlates better with the time series of dense water exported into the abyss, compared with using the density of the peak transformation, because it is only the denser subset of Dense Shelf Water that is able to overflow to the abyss. The choice of density threshold also ensures that the Dense Shelf Water formation metric is always located on the downwelling/convergent (i.e. higher density) side of the peak surface water mass transformation, even in years when the peak surface water mass transformation shifts to a higher density.

The Dense Shelf Water formation time series was averaged over the preceding four years, as this provides the best match for the bottom water outflow down and along the continental slope (Figure S5b). The annual time series of Dense Shelf Water formation is quite noisy (orange dots in Figure S5b). In contrast, the Dense Shelf Water outflow (green line in Figure S5b, as measured by the passive tracer concentration at the ocean floor, averaged between the 1500 m and 3500 m isobaths on the western Weddell Sea continental slope (63-70°S)), is smoother and represents the integrated behaviour of the Dense Shelf Water formation over multiple preceding years. This choice is also physically justified because the dense waters on the continental shelf can be stored in a reservoir and take several years to overflow.

Text S4: Statistical Analysis

There is a high degree of autocorrelation in the time series of temperature and dense water formation shown in Figure 1c due to the low frequency variability. Correlation coefficients are therefore calculated using the effective sample size: $N_{eff} = N(1 - r_1 r_2)/(1 + r_1 r_2)$, where N is the complete sample size (number of years) and r_1 and r_2 are the autocorrelations of the two individual time series at a lag of 1 year. The significance value for the correlation coefficient between the two time series, r, is calculated by comparing the t-statistic ($r\sqrt{N_{eff}}/\sqrt{1-r^2}$) to the critical values of the student's t-distribution with ($N_{eff}-1$) degrees of freedom.

References

Griffies, S. M. (2012). *Elements of the Modular Ocean Model (MOM): 2012 release with updates (GFDL Ocean Group Technical Report No. 7).* Princeton, USA: NOAA/Geophysical Fluid Dynamics Laboratory, https://mom-ocean.github.io.

Hunke, E. C., Lipscomb, W. H., Turner, A. K., Jeffery, N., & Elliott, S. (2012). *CICE: The los alamos sea ice model documentation and software user's manual.* Princeton, USA: Technical report, Los Alamos National Laboratory.

Newsom, E. R., Bitz, C. M., Bryan, F. O., Abernathey, R., & Gent, P. R. (2016). Southern Ocean deep circulation and heat uptake in a high-resolution climate model. *J. Clim.*, *29*, 2597-2619.

Roquet, F., Charrassin, J.-B., Marchand, S., Boehme, L., Fedak, M., Reverdin, G., & Guinet, C. (2011). Delayed-mode calibration of hydrographic data obtained from animal-borne satellite relay data loggers. *J. Atm. Oceanic. Tech.*, *28*, 787-801.

Solodoch, A., Stewart, A. L., Hogg, A. M., Morrison, A. K., Kiss, A. E., Thompson, A. F., ... Cimoli, L. (2022). How does Antarctic Bottom Water cross the Southern Ocean? *Geophys. Res. Lett.*, *49*.

Stewart, K., Kim, W., Urakawa, S., Hogg, A., Yeager, S., Tsujino, H., ... Danabasoglu, G. (2020). JRA55-do-based repeat year forcing datasets for driving ocean – sea-ice models. *Ocean Model.*, *147*, 101557.

Treasure, A., Roquet, F., Ansorge, I., Bester, M., Boehme, L., Bornemann, H., ... de

Bruyn, P. (2018). Marine Mammals Exploring the Oceans Pole to Pole: A review of the MEOP consortium. *Oceanography*, *30*, 132-138.

Tsujino, H., Urakawa, L. S., Griffies, S. M., Danabasoglu, G., Adcroft, A. J., Amaral, A. E., ... Yu, Z. (2020). Evaluation of global ocean–sea-ice model simulations based on the experimental protocols of the Ocean Model Intercomparison Project phase 2 (OMIP-2). *Geosci. Model Dev.*, *13*, 3643–3708.

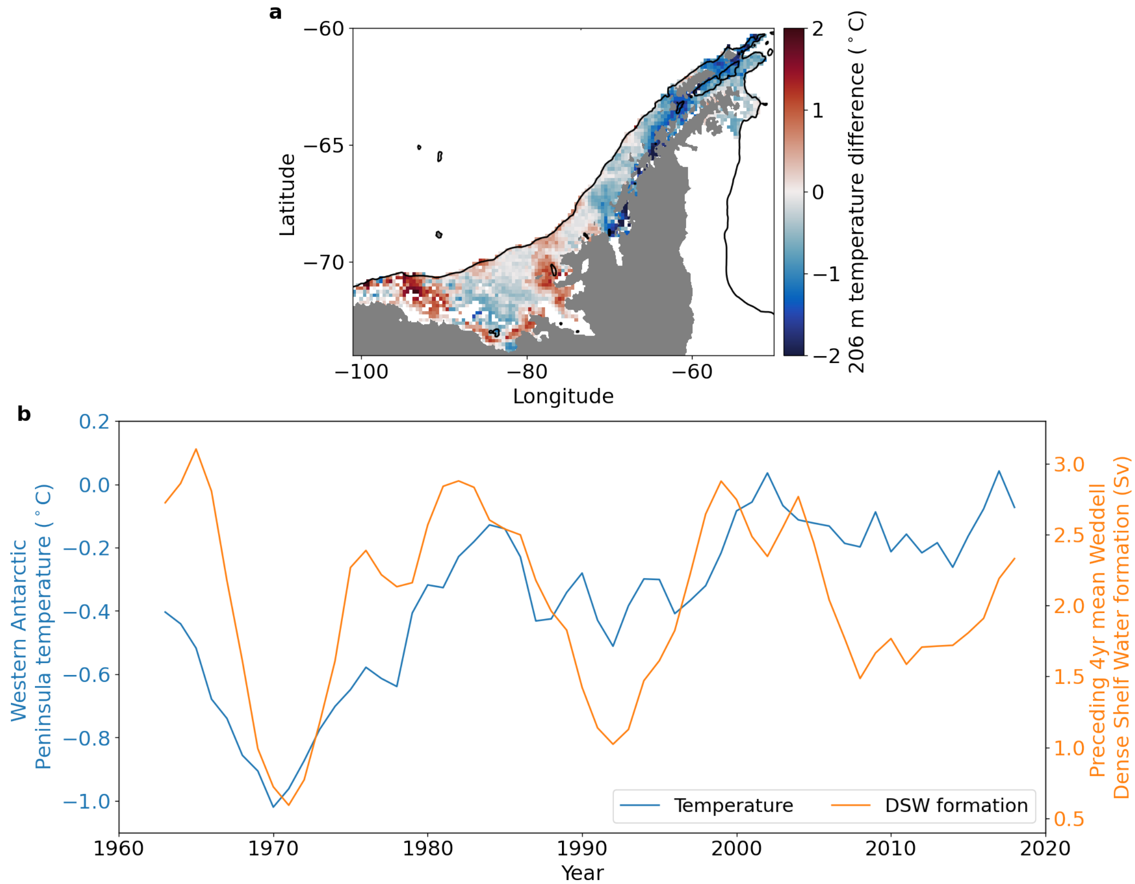

Figure S1. a) The difference in shelf conservative temperature at 206 m depth between the observed seal data and the historical simulation, as shown in Figure 1a,b. The model is subsampled spatially and temporally to match the seal observations, which cover the period 2005-2015. The black line shows the 1000 m isobath, and white areas on the shelf indicate no seal data is available. b) Identical to Figure 1c, except that the western Antarctic Peninsula ocean temperature (blue line) has not been detrended and the mean has not been subtracted. Simulated depth averaged western Antarctic Peninsula ocean temperature is shown in blue. Weddell Sea dense water formation averaged over the preceding 4 years is shown in orange. The blue and orange lines are calculated over the respective regions in the inset map in Figure 1d.

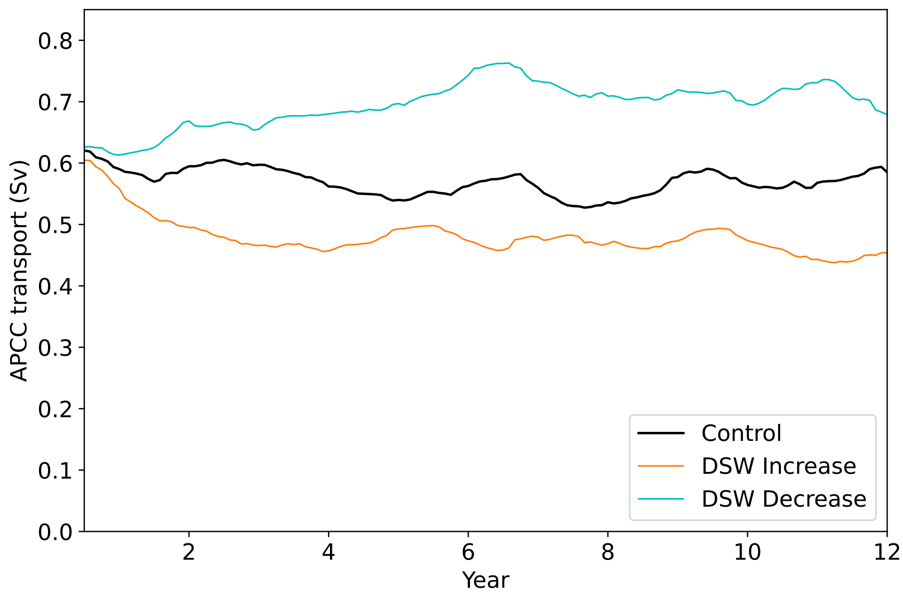

Figure S2. Time series of vertically integrated southward meridional transport in the Antarctic Coastal Current at 67°S along the western Antarctic Peninsula, for the control simulation (black), and perturbation simulations with increased (orange) and decreased (blue) Dense Shelf Water formation. Transport was cumulatively summed from the coast to the shelf break, with the maximum value of transport selected at each time. A 12 month rolling mean has been applied to remove the large seasonal cycle.

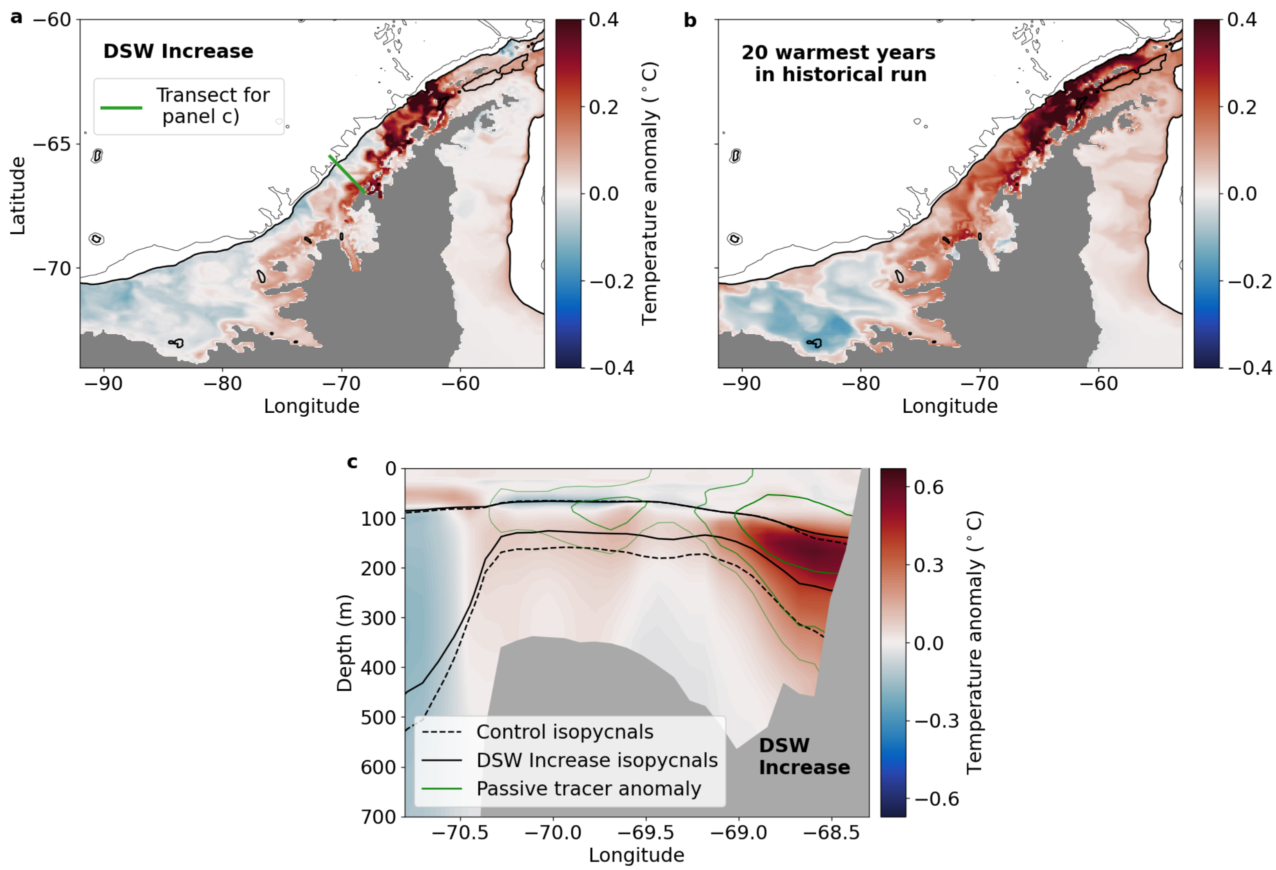

Figure S3. Identical to Figure 3a,b,d, except for warm anomaly cases. Depth averaged temperature anomaly over the continental shelf in (a) the simulation with increased Dense Shelf Water formation, relative to the control simulation and averaged over years 5-10, and in (b) the interannually forced historical simulation, averaged over the 20 warmest years in the detrended time series shown in Figure 1. In (a-b), thick and thin black contours show the 1000 m and 3000 m isobaths respectively. (c) Temperature anomaly following the increase in Dense Shelf Water formation, along a transect centred on 66°S (green line in (a)), and averaged over years 5-10. Black lines in (c) show isopycnals of potential density, $\rho_0 = 1027.6$ and $1027.78\ \mathrm{kgm^{-3}}$, in the control simulation (dashed) and when Dense Shelf Water formation is increased (solid) simulations. Green lines in (c) show passive tracer concentration anomalies of -0.03, -0.05 and -0.1 (light to dark).

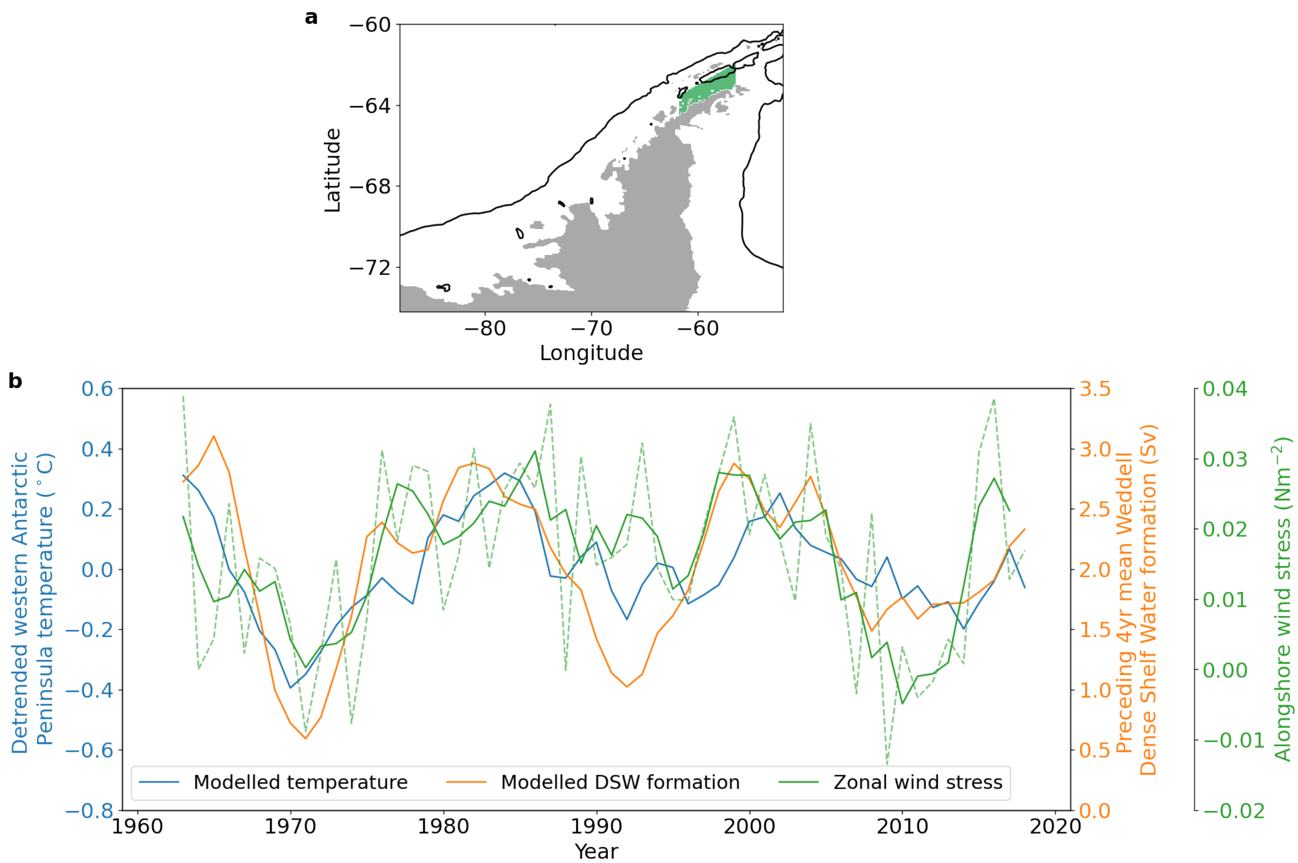

Figure S4. a) Map showing the region where the along-shore wind stress is analysed. b) Identical to Figure 1c, with the addition of the green lines showing variability in along-shore (north-eastward) wind stress averaged over the region shown in a). The wind stress has been detrended. The dashed green line shows annual averaged wind stress and the solid green line has a 3 year rolling mean applied.

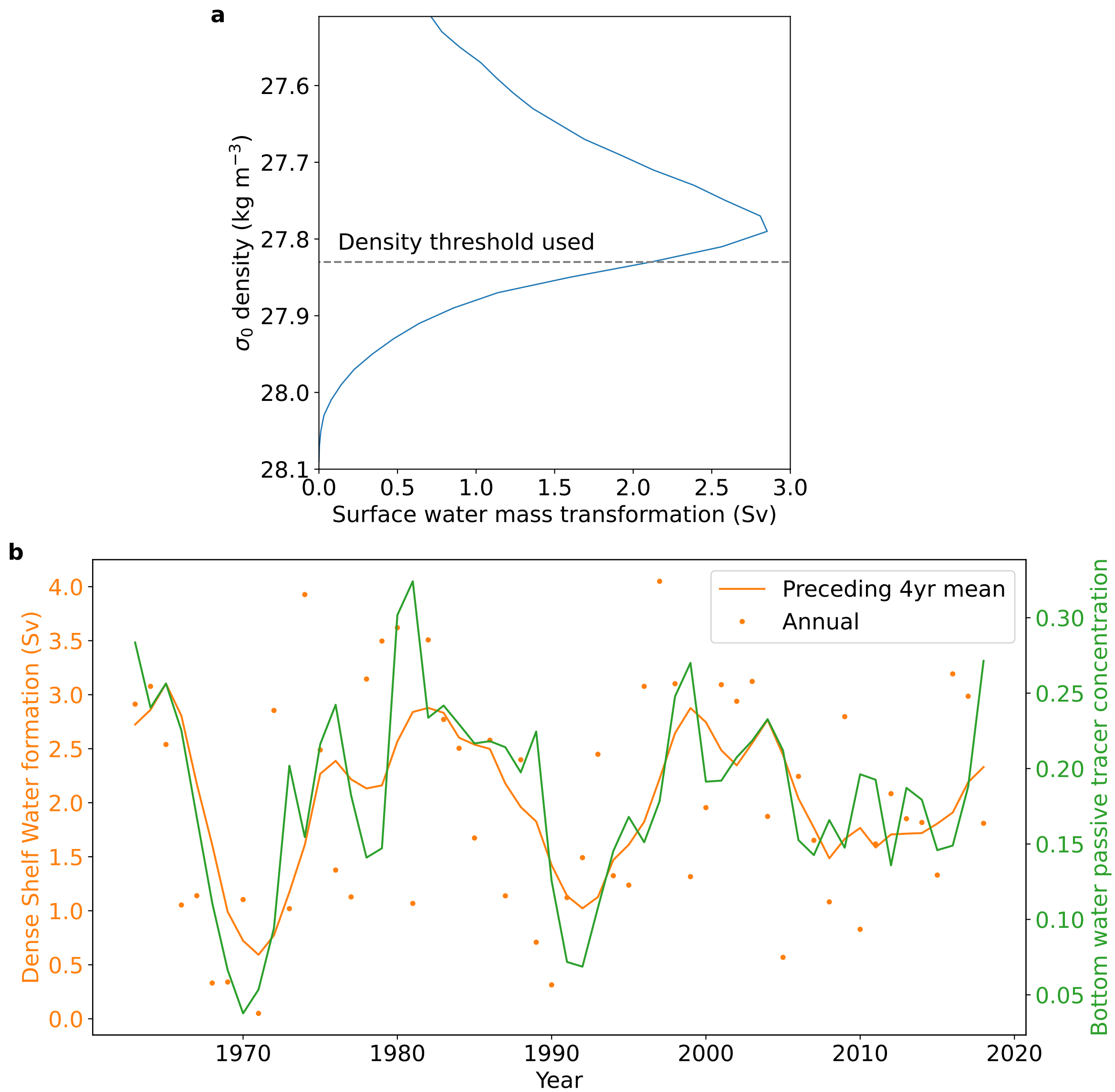

Figure S5. Choices made in the calculation of the Dense Shelf Water formation metric. a) Surface water mass transformation averaged over the historical simulation, and integrated over the Weddell Sea continental shelf (orange region shown in Figure 1d). The dashed line shows the density threshold used for the Dense Shelf Water formation calculation. b) Dense Shelf Water formation (orange), at annual temporal resolution (dots), and averaged over the preceding four years (solid; identical to the orange line in Figure 1d). The green line shows passive tracer concentration at the ocean floor, averaged between the 1500 m and 3500 m isobaths on the western Weddell Sea continental slope (63-70°S).